Comparative assessment of SIDC and SAM algorithms for soil classification using Sentinel-2 spectral reflectance: A case study from Kirkuk Province, Iraq

Hawar Abdulrzaq Sadiq Razvanchy

[1]Department of Soil and Water, College of Agricultural Engineering Sciences, Salahaddin University-Erbil, 44002 Erbil, Iraq
hawar.sadiq@su.edu.krd

Keywords: Soil Classification, Remote Sensing, SIDC, SAM, Spectral Reflectance

Abstract

This study evaluates and compares two remote sensing algorithms the Spectral Information Divergence Classification (SIDC) and the Spectral Angle Mapper (SAM) to determine their effectiveness in classifying soils based on spectral reflectance in Kirkuk Province, Iraq. Ten soil samples were collected from various locations representing the main soil types of the area. Laboratory analyses were performed to measure key soil properties such as texture, pH, electrical conductivity, and organic matter. While, spectral data (350–2500 nm) were obtained using an ASD FieldSpec3 spectroradiometer. These data were integrated with atmospherically corrected Sentinel-2 images and processed using ENVI software. The SIDC algorithm has been successfully classified a larger portion of the area but showed some confusion between soils and other land features. In contrast, SAM produced clearer and more accurate soil boundaries and it left a larger portion of the area unclassified. Validation using field data and visual comparison indicated that SAM achieved a higher accuracy (60%) than SIDC (10%). The SAM demonstrated greater precision in distinguishing soil types while SIDC provided wider coverage.

1. Introduction

The soil classification has a significant role in land evaluation and agricultural planning . Precise isolation of soils is important for improving agricultural productivity, water resource management, and sustainable land use [1,2]. Traditional soil survey method is cost and labor intensive. Also it depends deeply on field sampling and laboratory analysis [3]. But in remote sensing there is powerful way that has quick and effective properties [4,5] . Remote sensing depends on the reflectance data across narrow and continuous spectral bands, make it possible to predect soil properties such as texture, organic matter, and mineral composition [6].

It is kind of challenge to find a suitable and reliable soil classification methods that helps to differentiaite soils properly based on their spectral reflectance.

ISSN 2072-3857

Among the widely applied approaches are the Spectral Information Divergence Classification (SIDC) and the Spectral Angle Mapper (SAM), both designed to assess spectral variability in soils [7].

The SIDC calculates the divergence or differences between the soil reflectance from satellite image and the spectral reflectance taken from spectroradiometer. This makes the method highly sensitive to subtle differences in spectral signatures, thereby enhancing its ability to separate soil types with overlapping reflectance characteristics [8]. While the SAM calculate and measure the angle between the two mentioned spectral and depending mainly on the spectral shape. Because of the SAM algorithms ability to reduce the illumination effects makes it a strong tool for soil classification under different field conditions [9].

Kirkuk province is located at the north of Iraq and it has a different soil types. The soils in this area formed under different topography, geology, and land use. Understanding the spectral characteristics and spatial distribution of these soils is necessary for making better and sustainable agricultural practices [10]. In the study area there are very limited research in terms of comparing the different algorithms of the classification of soils based on remote sensing.

The first objective of this study is to evaluate the performance of each one of the SIDC and SAM in soil classification in Kirkuk province using spectral reflectance. The second one is comparing these two methods and select the most reliable one. The findings are expected to assist researches and decision-makers in adopting most effective method.

2. Methodology

2.1 Study Area

Kirkuk province is the study area and it is located in the north of Iraq. It located between latitude of 34°50′ N to 36°00′ N and longitude of 43°25′ E to 44°50′ E. It covers an area of 9,679 km² and is bordered by Erbil to the north, Sulaymaniyah to the east, Salahaddin to the west, and Diyala to the south. Kirkuk city is the provincy capital (Figure 1) [11]. The Kirkuk province is divided into four districts of Kirkuk, Daquq, Hawija, and Dibis. Each one of this districts has a large agricultural areas that play a significant role in Iraq's food production [12]. The topography in the study area is generally flat to gently undulating. The elevations ranging from 150 to 400 meters. There is sloping from southwest and northeast hills around Altun Kupri and Dibis toward the extensive agricultural plains of Daquq and Hawija [13]. The climate is semi-arid continental, characterized by hot, dry summers with temperatures becomes over 40 °C. With cool and wetter winters where temperatures can fall to 5 °C. The average annual rainfall is around 300-450 mm falling almost between November and April [14]. The most strategic crops in this province are wheat and barley [15]. The Lesser Zab River is the most important surface water source that using for irrigation [16].

ISSN 2072-3857

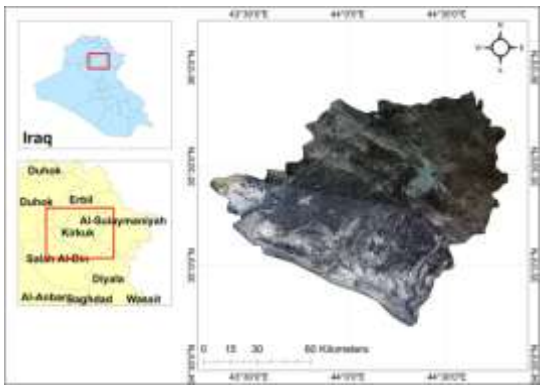

Figure 1: The study area location

2.2 Soil Sampling

Ten distinct soil types were identified in the study, based on previous soil surveys, spatial variation, and field investigations (Figure 2). All samples have been collected in May of 2024. In the field surface composite soil samples from 0 to 30 cm depth were taken. At each site, GPS coordinates have been recorded using a Garmin eTrex Solar device. The collected samples were carefully labeled, stored, and transported for subsequent laboratory analyses and spectral measurements.

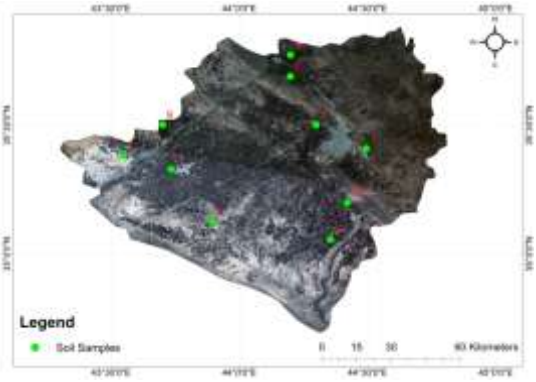

Figure 2: The soil samples locations

Table 1: Names and locations of the soil samples

No.	Name	Latitude (°)	Longitude (°)	Elevation (m)
1	Laylan	35.409 831	44.494 443	265
2	Kirkuk	35.502 087	44.299 106	288
3	Daquq	35.056 234	44.355 657	205
4	Rashad	35.124 910	43.896 171	192
5	Altun Kupri	35.774 365	44.199 156	272
6	Dibis	35.690 938	44.199 093	245
7	Hawija	35.329 109	43.734 699	191
8	Riyadh	35.383 956	43.550 332	185
9	Hawija	35.502 492	43.701 450	198
10	Taza Khurmatu	35.199 446	44.421 816	210

2.3 Laboratory Analysis

Soil samples from the 10 selected sampling sites were air-dried, gently ground, and sieved through a 2 mm mesh to obtain a homogeneous material for the laboratory and spectral measurement using standard procedure [17]. Several physicochemical properties of particle size distribution (PSD), soil pH, organic matter (OM), and electrical

ISSN 2072-3857

conductivity (EC) have been performed in the laboratory to support spectral classification and validate results according to the following methodologies. The selection of these parameters as the primary laboratory analyses was driven by their significant role in defining soil fertility and spectral behavior.

2.3.1 Particle Size Distribution (PSD)

It has a strong influence on water retention, nutrient availability, and surface reflectance, making it a important parameter for soil using remote sensing [4]. Determined using the hydrometer method [18].

2.3.2 Soil pH

Soil pH is represent chemical reactivity, nutrient solubility, and overall agricultural suitability. Its impact on spectral signatures has been documented in semi-arid soils, including those comparable to conditions in northern Iraq [19]. Measured using a HANNA HI9814 pH meter with a 1:1 soil-to-water ratio.

2.3.3 Electrical Conductivity (EC)

The electrical conductivity was included to account for soil salinity, a common limitation in arid and semi-arid agriculture. Salinity not only restricts crop productivity but also modifies spectral reflectance patterns, particularly within the shortwave infrared domain [20].Measured using an HANNA HI9814 EC meter with a 1:1 soil-to-water ratio.

2.3.4 Soil Organic Matter (OM)

The organic matter content serves as a key indicator of fertility and soil carbon content, while also affecting soil color and light absorption features in the visible and near-infrared regions [17]. Estimated using the Walkley-Black wet oxidation method.

These four properties provide a comprehensive assessment of the physical and chemical conditions of soils in the study area. At the same time, they are directly related to the spectral variability that supports classification approaches such as SAM and SIDC.

2.4 Spectral Data Acquisition

The spectral measurement for the ten selected samples have been performed. Laboratory spectral reflectance of each prepared sample was measured across the visible-near infrared and shortwave-infrared regions (VNIR-SWIR, 350-2500 nm) using a calibrated ASD FieldSpec3 spectroradiometer (350-2500 nm). Measurements were taken using a stable halogen lamp and a Spectralon white reference for reflectance calibration for each sample, ten scans were recorded and averaged to reduce noise. Raw spectral were trimmed to remove low signal regions (typically <400 nm and >2450 nm), and smoothed (Savitzky–Golay) and normalized to reduce variability caused by particle size and illumination differences [4]. The processed spectral data were imported into ENVI 5.3 software to build a spectral library of the ten soil types.

ISSN 2072-3857

2.5 Remote Sensing Data

2.5.1 Preprocessing

A mosaicked of two Sentinel-2 satellite images covering Kirkuk province were acquired for May 2024. Both of radiometric correction and atmospheric correction were performed on the satellite images using Fast Line of sight Atmospheric Analysis of Spectral Hypercubes (FLAASH) module from ENVI software to convert digital numbers (DN) into surface reflectance. Images were georeferenced using field GPS points and a digital elevation model (DEM) for the study area to ensure spatial accuracy. The image was subset to cover only Kirkuk province to optimize computational efficiency.

2.6 Classification Algorithms

2.6.1 Spectral Angle Mapper (SAM)

SAM is a physically based spectral classification technique that computes the angle between the spectral vectors of an unknown spectrum and the reference spectrum in an n-dimensional space to assess how similar they are. The soil spectral library was used as input for the SAM classifier in ENVI software. Pixels were assigned to the closest soil type using a threshold angle of 0.1 radians, which was determined through trial and error. The following equations illustrate how this algorithm operates:

$$s = [s1, s2, s3, \dots, sn], \qquad t = [t1, t2, t3, \dots tn] \quad \dots\dots\dots (1)$$

$$\theta(s,t) = \cos^{-1}\left(\frac{\sum_{i=1}^{N} siti}{\sqrt{\sum_{i=1}^{N} s_i^2}\sqrt{\sum_{i=1}^{N} t_i^2}}\right) \dots\dots\dots (2)$$

2.6.2 Spectral Information Divergence Classification (SIDC)

SIDC treats two spectrum as probability distributions and calculates their probabilistic divergence. It can distinguish between soil classes with overlapping reflectance and is sensitive to subtle variations in spectral shape. The SIDC classifier was used in ENVI using the same spectral library as the reference input. A 0.05 divergence threshold was applied. The algorithm on which SIDC is based is shown by the following equations:

$$s = [s1, s2, s3, \dots, sn], \qquad t = [t1, t2, t3, \dots tn] \quad \dots\dots\dots (3)$$

$$pi = \frac{si}{\sum_{j=1}^{N} sj}, \qquad qi = \frac{ti}{\sum_{j=1}^{N} ti} \dots\dots\dots (4)$$

$$D(p||q) = \sum_{i=1}^{N} pi \log\left(\frac{pi}{qi}\right), \quad D(q||p) = \sum_{i=1}^{N} qi \log\left(\frac{qi}{pi}\right) \quad \dots\dots\dots (5)$$

$$SIDC\,(s,t) = D(p||q) + D(q||p) \dots\dots\dots (6)$$

2.7 Data Analysis and Visualization

In order to assess the effectiveness of the two algorithms, SAM and SIDC, and to produce an interpretable soil classification map for the study area, the analysis of the spectral and classification results comprised a number of sequential steps. The outcomes were then post-processed to guarantee cartographic

ISSN 2072-3857

comprehension and eliminate noise. To make interpretation easier, visualization was done. After being created in ENVI, the finished soil classification maps were exported as GeoTIFFs so that ArcGIS Pro could be used for additional cartographic design . To improve visual differentiation, a uniform color scheme was used on all maps, giving each of the ten soil types a unique hue. Continuous similarity layers from SAM (spectral angle) and SIDC (divergence values) were normalized and displayed as grayscale or graduated color rasters to convey spatial uncertainty, emphasizing regions with high versus low confidence in classification outcomes . These visualization products will improve the findings readability and allow for a comparative analysis of algorithmic performance and audience visions, which supports the assessment of spectral mapping as a soil resource assessment tool in semi-arid areas like Kirkuk. To identify the more dependable algorithm for soil type discrimination, statistical comparisons of classification accuracies were conducted.

3. Results and Discussion

3.1 SIDC

The SIDC methodology successfully delineated different soil classes across the study area. The results (Table 2 and Figure 3) indicate that class S1 dominated, covering an area of 8,027.32 km². The other classes of S2 (1,105.39 km²), S3 (2,023.48 km²), and S6 (2,307.88 km²) have medium occubation following by the classes of S5 (578.44 km²) and S7 (224.36 km²). While the classes of S8 and S10 represent very limited extents of 22.63 and 2.12 km² respectively. On the other side, the classed of S4 and S9 occupies only 0.51 and 0.59 km², indicating that these soil type are rare. The Unclassified class occupy 3,974.22 km² which is unclassified pixels or it does not match any of these ten spectral signisure according to the SIDC algorithm. The SIDC-derived soil classes demonstrated strong correspondence with the measured physicochemical properties of soils at the sampled locations (Table 4). The dominant classes (S1 and S6, covering over 10,000 km²) were largely associated with loam and clay loam textures (Laylan, Daquq, Rashad, Altun Kupri, Hawija, Taza Khurmatu). These soils showed moderate pH values (7.3-7.5), relatively higher organic matter content (1.6-2.3%), and low to moderate EC (0.7-1.3 dS/m), which together enhance spectrals sensitivity. Loam and clay-rich soils tend to retain more moisture and organic matter producing darker reflectance signatures in the visible and near-infrared regions [21]. In contrast, classes such as S2 and S5, covering smaller areas corresponded mostly to sandy loam soils (Kirkuk, Dibis, Riyadh). These exhibited slightly more alkaline conditions (pH 7.6-7.8), lower organic matter (0.9-1.2%), and somewhat higher EC (1.1-1.5 dS/m). Sandy soils generally show higher reflectance due to low organic matter and weak water-holding capacity [22], which explains their weaker spectral distinctiveness. The classes such as S8, S9, and S10 represent soils with distinct textures where spectral overlap reduces classification accuracy. The large unclassified area (3,974.22 km²) can be attributed to small mixed areas that

cannot be tend to any of the spectrum as a spectral confusion between loam and sandy loam soils which is kind of challenge in in this kind of soil studies [6]. It indicates that soil spectral classes are primarily driven by texture, organic matter, and salinity, with loam and clay loam soils showing clearer spectral signatures than sandy soils, supporting the robustness of the SIDC methodology.

Table 2: The area occupied by each spectral signature using SIDC

Area (%)	Area (km^2)	Classes
21.756	3,974.22	Unclassified
43.945	8,027.32	S1
6.051	1,105.39	S2
11.077	2,023.48	S3
0.003	0.51	S4
3.167	578.44	S5
12.634	2,307.88	S6
1.228	224.36	S7
0.124	22.63	S8
0.003	0.59	S9
0.012	2.12	S10

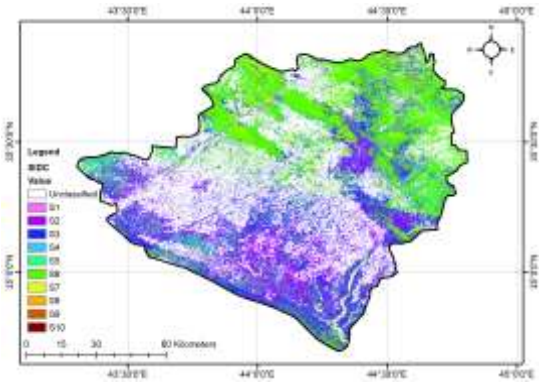

Figure 3: The spatial distribution of the isolated classes using the SIDC algorithm

3.2 SAM

The spectral classification of soils based on the SAM algorithm performed with a significantly different distribution of classes compared to SIDC, with a large area of the study area falling into the Unclassified category (15,330.36 km²) (Table 2 and Figure 4). This suggests that SAM, being more accurate in its pixel assignment, struggles with mixed spectral and overlapping soil signatures [23]. Among the classified soils the classes of S3 (1,849.68 km²) and S5 (3,76.34 km²) were the most covered area classes. While the classes of S1, S2, S6, and S7 covered smaller areas relatively which ranging between 36-247 km². The other soil classes such as S4, S8, and S9 were very low area occupation each covering less than 5 km². Whereas the classes of S10 occupied 61.61 km². These behaviors of isoilation of the soil classes can be linked with field measured soil properties (Table 4). The classes of S3 and S5 are dominant and they correspond to clay loam and loam content in the soils (Daquq, Rashad, Hawija, Altun Kupri, Taza Khurmatu). These soils exhibit moderate pH (7.3-7.5), high organic matter content (1.6-2.3%), and relatively low EC (0.7-1.3 dS/m). The stronger representation of these soils under the SAM classification reflects their more consistent spectral behavior as clay and organic matter influence absorption features in the shortwave infrared region [6]. In contrast, sandy loam soils (Kirkuk, Dibis, Riyadh), characterized by slightly higher pH (7.6-7.8), lower organic matter (0.9-1.2%), and higher EC (1.1-1.5 dS/m), were less detected as shown in classes of S2, S6, and S7. Sandy soils

ISSN 2072-3857

tend to exhibit higher reflectance and weaker diagnostic absorption features, which reduces their separability with SAM [22].

Table 3: The area occupied by each spectral signature using SAM

Area (%)	Area (km^2)	Classes
83.924	15330.36	Unclassified
0.197	36.04	S1
1.008	184.14	S2
10.126	1849.68	S3
0.001	0.0981	S4
2.060	376.34	S5
1.353	247.18	S6
0.961	175.51	S7
0.025	4.48	S8
0.008	1.51	S9
0.337	61.61	S10

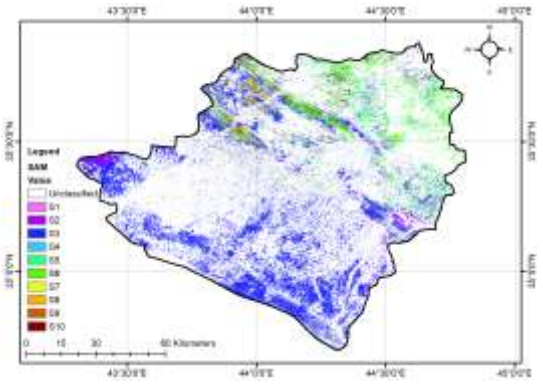

Figure 4: The spatial distribution of the isolated classes using the SAM algorithm

3.3 Comparative Analysis of SIDC and SAM Methodologies

The unclassified area class from SAM compared to SIDC indicates that SAM is more sensitive to spectral variability and may reject mixed or unclear areas rather than forcing them into a class. This is particularly relevant in transitional zones between sandy loam and loam soils, where spectral confusion is greatest. While SAM was effective in identifying clay loam and loam soils with clearer spectral signatures, it left a significant portion of the study area unclassified, suggesting that SIDC may offer a more comprehensive mapping approach in mixed properties. The application of SIDC and SAM revealed large differences in soil classification performance across the study area. SIDC alghorith successfully classified a larger portion of the landscape into soil categories with relatively low unclassified areas (3,974.22 km^2). Nevertheless, this bigger coverage area comes due to spectral mixing. The soils are sometimes misclassified with spectral similar features such as urban areas and bare rock surfaces. The spectral confusion is a common phenomenon of divergence-based classifiers, as they depend on pixel similarity measures that are sensitive to noise and spectral overlaps [24]. In the opposite, SAM result much larger unclassified area (15,330.36 km^2), produced cleaner separations between soil classes and minimized confusion with non-soil features. This is because SAM calculates the spectral angle between the pixel spectrum and reference spectrum making it less sensitive to albedo differences and illumination effects [25]. As a result, SAM more effectively separated clay loam and loam soils (S3 and S5) which are spectrally dependable due to their higher clay and organic matter content. By comparison, SIDC tended to overestimate the extent of sandy soils

ISSN 2072-3857

and transitional or mixed areas. This is partly due to spectral mixing with urban pixels and bare soil or rock surfaces. From an agricultural and environmental monitoring perspective, SAM is valuable because accurate soil monitoring is more critical than complete coverage. For instance, in areas such as Daquq, Rashad, and Taza Khurmatu, SAM clearly delineated clay loam soils with moderate pH (7.3-7.5), higher organic matter (1.6-2.3%), and low EC (0.7-1.3 dS/m), which are essential indicators of soil fertility. These properties strongly influence spectral responses in the visible, near-infrared, and shortwave infrared ranges [6]. On the other hand, SIDC often misclassifies these fertile areas due to the spectral overlap with nearby urban and built-up areas, which leading to confusions in land evaluation at the end.

Table 4: The physicochemical properties of the soil samples

EC (dS/m)	OM (%)	pH	Soil Class	PSD (%)			Location Name	No.
				Clay	Silt	Sand		
0.9	1.8	7.4	Loam	20	35	45	Laylan	1
1.1	1.2	7.6	Sandy Loam	20	25	55	Kirkuk	2
0.8	2.0	7.3	Clay Loam	25	40	35	Daquq	3
1.3	1.6	7.5	Clay Loam	30	30	40	Rashad	4
0.7	2.1	7.2	Loam	15	35	50	Altun Kupri	5
1.4	1.0	7.7	Sandy Loam	15	25	60	Dibis	6
1.0	1.9	7.4	Clay Loam	30	32	38	Hawija	7
1.5	0.9	7.8	Sandy Loam	15	20	65	Riyadh	8
0.8	2.3	7.3	Loam	18	34	48	Hawija	9
1.2	1.7	7.5	Clay Loam	30	28	42	Taza Khurmatu	10

ISSN 2072-3857

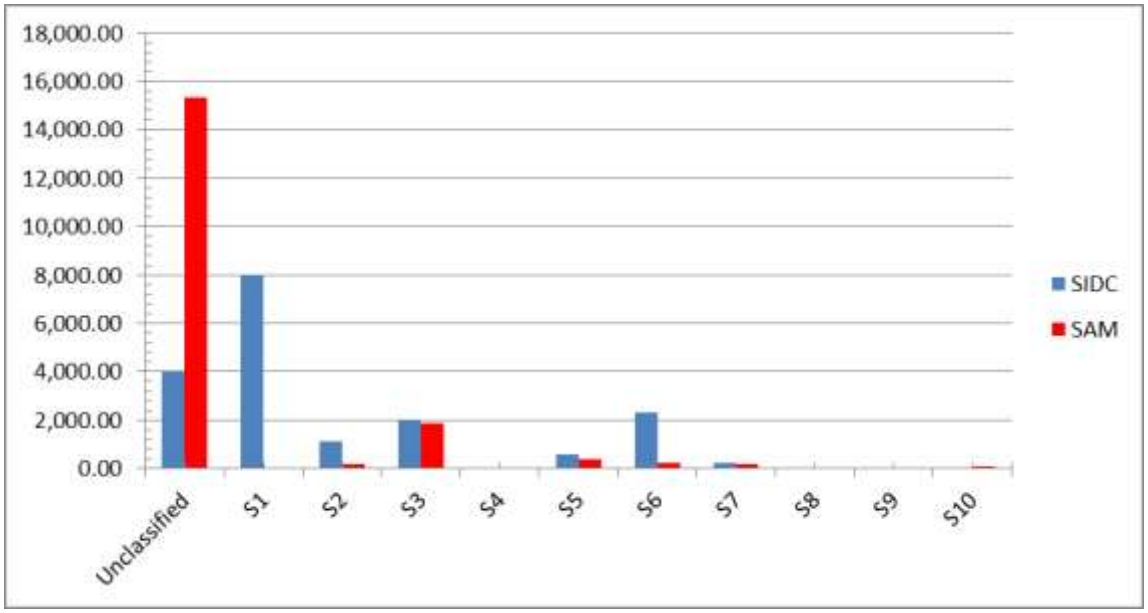

Figure 5: Area occupied comparison between SIDC and SAM

4. Result Validation

4.1 Visual Result Validation

To ensure that the soil classification results are accurate, a visual comparison was performed between the satellite images (true color composite) and the soil map produced using the SAM algorithm (Figure 6). This approach helped evaluate how well the classified results matched the satellite images the comparison showed a strong agreement between the both. The areas that appeared light in the satellite images were correctly classified, while darker areas were also accurately identified. The SAM algorithm effectively separated these soil types by measuring the spectral angle between their reflectance patterns which made it particularly good at distinguishing small differences. Compared to the SIDC, SAM produced cleaner and more consistent boundaries with less confusion between soil and non-soil surfaces such as vegetation or urban areas.

This kind of visual validation is a common and reliable method in remote sensing studies [26]. By comparing the classified outputs directly with satellite images. It can be used to quickly assess whether the patterns produced by the algorithm reflect actual land surface characteristics [27]. In this study, the SAM-based classification for the study area closely matched the variation shown in the images. It suggesting that provides a realistic and dependable representation of soil variability. The validation results confirm that SAM is a strong and accurate technique for mapping different soil types based on their spectral signatures.

ISSN 2072-3857

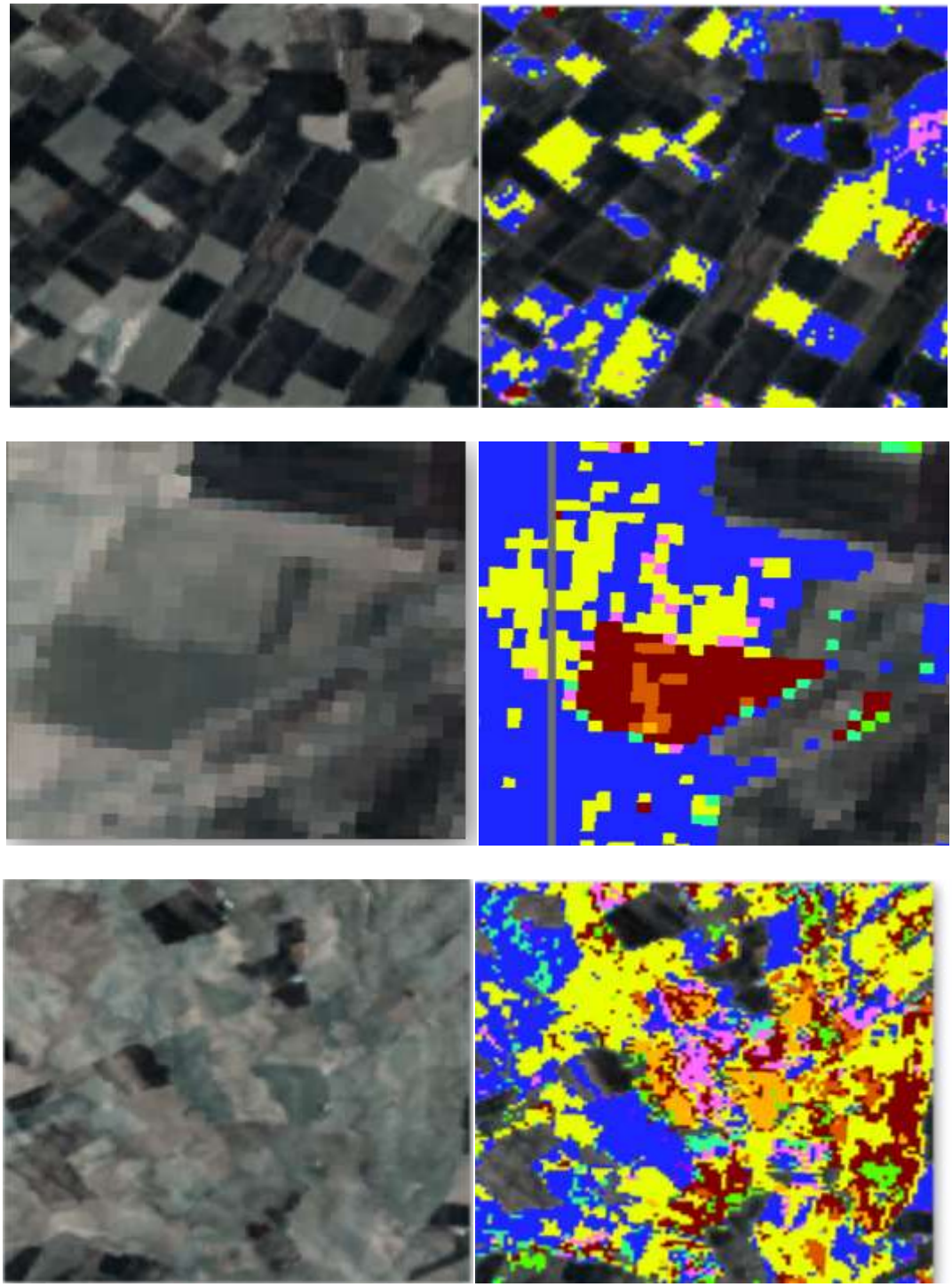

Figure 6: SAM-based maps visual result validation

ISSN 2072-3857

4.2 Statistical Result Validation

During the field work the real soil status of each of the ten points has been recorded. All the soil samples soil status were bare soils and they differed in terms of physical and chemical properties according to the field evaluation. The values of these points have been extracted (using the multi-value extraction function) from the produced maps that have been generated from both algorithms. Therefore, the values appear in the table 5 are the values of the exact and same locations where the spectral signature have been taken. The result shows that the SAM-based map matches 60% of the taken spectral reflectance with the soil samples location (soil classes). These differences returns to some reasons, the first one is that there is little class mixing especially in the locations of 2, 3, 6, and 7. Because the real or the matched classes are surrounding the real ones with a distance between 100-200 meters, and if the majority of the classes will be taken for the points of 2, 3, 6, and 7, the matching will reach 80%. The second reason is the number of taken spectral reflectances are relatively low. On the other side, the match ratio based on SIDC-generated map is significantly low (10%) in comparison with the SAM-based. This is due to the huge mixing up between classes and the similarity among soil reflectances which this algorithm couldn't separate them properly.

Table 5: Comparison between detected classes by both SAM and SIDC algorithms for the same locations

Classes from SAM map	Classes from SIDC map	Soil sample locations
1	3	1
2	5	2
3	2	3
4	3	4
5	6	5
6	6	6
6	3	7
3	3	8
3	3	9
NULL	NULL	10
60%	10%	Match ratio

5. Conclusion

The SIDC provides broader but noisier coverage, and SAM offers higher classification precision, especially in heterogeneous landscapes where soil features coexist with anthropogenic and natural non-soil surfaces. For robust soil mapping, a combined approach could be beneficial: using SIDC for initial area-wide soil separation, followed by SAM to refine the results and eliminate urban/rock interference.

ISSN 2072-3857

5. References

[1

] H. Jenny, *Factors of Soil Formation: A System of Quantitative Pedology*. New York: Dover Publications, 1994 (original work published 1941).

[2] FAO, *Status of the World's Soil Resources: Main Report*. Rome: Food and Agriculture Organization of the United Nations (FAO), 2015.

[3] A. B. McBratney, M. L. Mendonça Santos, and B. Minasny, "On digital soil mapping," *Geoderma*, vol. 117, no. 1–2, pp. 3–52, 2003.

[4] E. Ben-Dor, S. Chabrillat, J. A. M. Demattê, G. R. Taylor, J. Hill, M. L. Whiting, and S. Sommer, "Using imaging spectroscopy to study soil properties," *Remote Sensing of Environment*, vol. 113, pp. S38–S55, 2009.

[5] R. A. V. Rossel, D. J. J. Walvoort, A. B. McBratney, L. J. Janik, and J. O. Skjemstad, "Visible, near infrared, mid infrared or combined diffuse reflectance spectroscopy for simultaneous assessment of various soil properties," *Geoderma*, vol. 131, no. 1–2, pp. 59–75, 2010.

[6] S. Chabrillat, E. Ben-Dor, J. Cierniewski, C. Gomez, T. Schmid, and B. van Wesemael, "Imaging spectroscopy for soil mapping and monitoring," *Surveys in Geophysics*, vol. 40, no. 3, pp. 361–399, 2019.

[7] C.-I. Chang, "An information-theoretic approach to spectral variability, similarity, and discrimination for hyperspectral image analysis," *IEEE Transactions on Information Theory*, vol. 46, no. 5, pp. 1927–1932, 2000.

[8] Y. Chen, N. M. Nasrabadi, and T. D. Tran, "Hyperspectral image classification using dictionary-based sparse representation," *IEEE Transactions on Geoscience and Remote Sensing*, vol. 49, no. 10, pp. 3973–3985, 2011.

[9] F. D. van der Meer, "The effectiveness of spectral similarity measures for the analysis of hyperspectral imagery," *International Journal of Applied Earth Observation and Geoinformation*, vol. 8, no. 1, pp. 3–17, 2006.

[10] A. Abbas, N. Al-Ansari, and S. Knutsson, "Soil mapping and classification in Iraq using remote sensing and GIS techniques," *Journal of Earth Sciences and Geotechnical Engineering*, vol. 10, no. 4, pp. 41–56, 2020.

[11] N. Al-Ansari, S. Knutsson, and A. Ali, "Agricultural water management in Iraq," *Water Practice and Technology*, vol. 16, no. 2, pp. 389–401, 2021.

[12] CSO (Central Statistical Organization), *Kirkuk Governorate Statistical Yearbook*. Baghdad: Government of Iraq, 2020.

[13] R. Mahmood, G. Rasul, and N. Sadiq, "Climate change impacts on agriculture in Iraq," *Environmental Earth Sciences*, vol. 79, no. 9, p. 220, 2020.

[14] G. Rasul, H. Hussein, and M. Al-Dabbas, "Climatic variability and its impacts on agricultural productivity in northern Iraq," *International Journal of Climatology*, vol. 38, no. 4, pp. 2015–2027, 2018.

[15] FAO, *Irrigation in the Middle East Region in Figures: Iraq Country Report*. Rome: FAO AQUASTAT, 2019.

[16] UNESCO, *Groundwater Resources in Iraq: A Case Study of Kirkuk and Surroundings*. Paris: UNESCO-IHP, 2014.

ISSN 2072-3857

[17] E. Ben-Dor and A. Banin, "Near-infrared analysis as a rapid method to simultaneously evaluate several soil properties," *Soil Science Society of America Journal*, vol. 59, no. 2, pp. 364–372, 1995.

[18] G. Gee and J. Bauder, "Particle-size analysis," in *Methods of Soil Analysis: Part 1—Physical and Mineralogical Methods*, 2nd ed., SSSA Book Series, 1986.

[19] G. Zhang, X. Li, X. Wang, X. Han, and Z. Gong, "Spectral characteristics of soil pH and its estimation at different scales," *Geoderma*, vol. 314, pp. 221–231, 2018.

[20] J. Farifteh, F. van der Meer, C. Atzberger, and E. J. M. Carranza, "Quantitative analysis of salt-affected soil reflectance spectra: A comparison of two adaptive methods (PLSR and ANN)," *Remote Sensing of Environment*, vol. 110, no. 1, pp. 59–78, 2006.

[21] C. Gomez *et al.*, "Soil organic matter prediction by hyperspectral remote sensing: An application to Mediterranean soils," *Geoderma*, vol. 146, no. 3–4, pp. 417–423, 2008.

[22] V. L. Mulder *et al.*, "Spectral soil mapping: A review of challenges and opportunities," *Geoderma*, vol. 162, no. 3–4, pp. 295–310, 2011.

[23] F. A. Kruse, A. B. Lefkoff, J. W. Boardman, K. B. Heidebrecht, A. T. Shapiro, P. J. Barloon, and A. F. H. Goetz, "The spectral image processing system (SIPS) interactive visualization and analysis of imaging spectrometer data," *Remote Sensing of Environment*, vol. 44, no. 2–3, pp. 145–163, 1993.

[24] A. Plaza *et al.*, "Recent advances in techniques for hyperspectral image processing," *Remote Sensing of Environment*, vol. 113, pp. S110–S122, 2009.

[25] R. N. Clark *et al.*, "Imaging spectroscopy: Earth and planetary remote sensing with the USGS Tetracorder and expert systems," *Journal of Geophysical Research: Planets*, vol. 108, no. E12, 2003.

[26] D. Lu and Q. Weng, "A survey of image classification methods and techniques for improving classification performance," *International Journal of Remote Sensing*, vol. 28, no. 5, pp. 823–870, 2007.

[27] J. R. Jensen, *Introductory Digital Image Processing: A Remote Sensing Perspective*, 4th ed. Pearson, 2016.

ISSN 2072-3857